

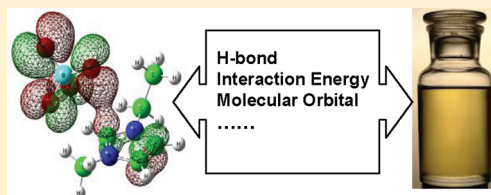
Understanding Structures and Hydrogen Bonds of Ionic Liquids at the Electronic Level

Kun Dong, Yuting Song, Xiaomin Liu, Weiguo Cheng, Xiaoqian Yao, and Suojiang Zhang*

State Key Laboratory of Multiphase Complex Systems, Institute of Process Engineering, Chinese Academy of Sciences, Beijing, 100190, P. R. China

S Supporting Information

ABSTRACT: Due to their unique properties, ionic liquids (ILs) have attracted the academic and industrial attentions. However, recent controversies have focused on what are the main forces to determine the behaviors of ILs. In this work, a detailed DFT calculation was carried out to investigate the intermolecular interactions in two typical ILs, [Emim][BF₄] and [Bmim][PF₆]. The results indicate that hydrogen bonds (H-bonds) are the major intermolecular structural feature between cations and anions. Although the electrostatic force remains the major noncovalent force (70% of the total energy by energy decomposition calculation), the interaction energies calculated at different theoretical levels indicate that H-bond and van der Waals interactions cannot be ignored. However, the H-bonded capacities from natural bond orbital (NBO) delocalization energies do not show the consistent changes in the total interaction energies and number of H-bonds. Based on the canonical orbitals analysis, it is found that the σ -type orbital overlap and the partial charges transfer between anion and cation, finally, result in the significant energy reduction and rationalize the preferable location of anion, which is an essential understanding for the interaction and structure in the ion pair. Additionally, the strong agreement between the experimental IR spectra and the calculated vibrations implies that the structures of the larger ion clusters provide a reasonable depiction for bulk ILs at room temperature condition.



INTRODUCTION

As novel and green class of chemical components, room temperature ionic liquids (RTILs) have gained increasing interest and attention in both academia and industries.¹ RTILs are typically composed of organic cations and inorganic anions and possess many unique properties, such as low melting points, negligible vapor pressures, high thermal stabilities, and non-flammability, which have shown potential applications in some chemical processes to replace volatile organic compounds (VOCs).^{2,3} An advantage of RTILs is the structural tunability by combining a large number of different cations with anions (it is evaluated that there are about a million possible pure ILs and 10¹⁸ ternary liquid mixtures).⁴ Obviously, it is very necessary for a chemical engineer to make such choices. However, in most cases blind choices may result in failure. A main point lies in the defective knowledge about the relationship between properties and structures of the synthesized RTILs, which usually can provides us the rational conducts for the experimental chemical processes, such as in the separation, catalysis, and even the synthesis of the new materials.⁴

The behavior of a solvent is usually determined by the intermolecular interactions. However, in RTILs, the ion interactions include the Coulombic force, dipole–dipole, dipole–induced dipole, dispersion, and hydrogen bond, which are very complicated and have not been unraveled completely up to now.^{5–7} Many experiments have been carried out to investigate the interactions between cations and anions among a series of ILs. Spectroscopic studies^{8–15} in many typical imidazolium-based ILs

have shown that noncovalent interactions determined the important properties of ILs. In 1986, Seddon et al. proposed that there existed H-bonds in [Emim]I ion pair,¹⁶ and the continued discussion on the noncovalent interactions has shifted to the function of H-bond and its effect on properties of ILs. X-ray and IR spectra have also demonstrated unambiguously that H-bonds are the important noncovalent interactions between anion and cation in the typical imidazolium-based ILs.^{12,15,17,18}

The identification of H-bonds in the imidazolium-based ILs can be made by substituting for a proton using a –CH₃ group, which results in the complete disappearance of the bands associated with H-bonds. Combining far-IR, THz, and single-crystal X-ray diffraction, Ludwig et al. had demonstrated that the bands related to H-bonds disappeared in [Emim][Tf₂N] when the proton atoms on imidazolium-ring were replaced by the –CH₃ groups.^{19–21} With increasing abilities and strengths of H-bonds, the [Tf₂N][–] anion was found in the *cis* conformation. Switching off the local interactions leads to the energetically favored *trans* conformation. The structural shift caused by H-bonds has a significant effect on ILs' properties, such as melting points and viscosities.

Although these experiments have provided a lot of information about the structures of ILs, it is still a great challenge to understand these ionic compounds at the molecular level, and the H-bonded structures are blurred too.²² Theoretical

Received: June 9, 2011

Revised: December 23, 2011

Published: December 27, 2011

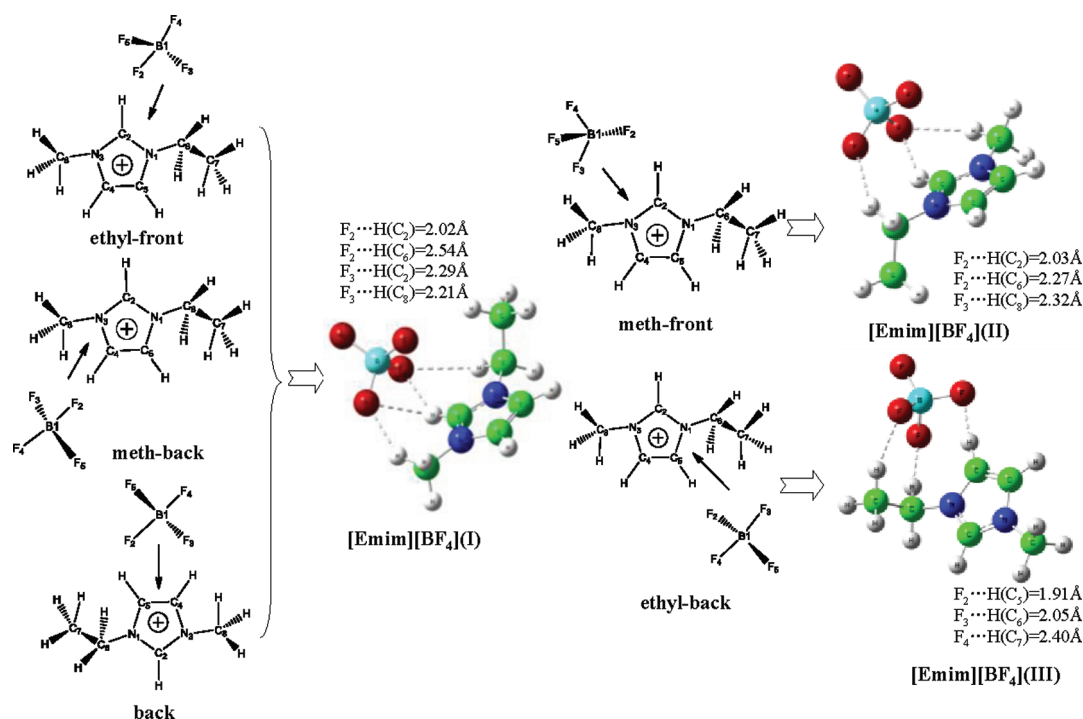


Figure 1. Optimized structures of the [Emim][BF₄] ion pair when the anion is located at five different positions of cation. The arrows represent the initial locations of the anion. The dashed lines note the H-bonds formed in the ion pairs. C atoms (green), N atoms (blue), H atoms (gray), F atoms (brown), B atoms (sky-blue) are shown by the different colors for clarity.

calculations can compensate the defects of the experiments and provide some accurate information about the relationship between structures and properties of ILs. Molecular dynamics (MD) and Monte Carlo simulations as two popular methods have been used to investigate the ions arrangements and thermodynamic properties in the pure bulk ILs and the solvated species.^{23–28} However, a key drawback of the simulations is the strong dependence on the quality of potential functions and the charges associated with each atom or group. There are still challenges in developing the predictive and transferable force fields. An obvious example is the [Bmim]Cl. The different models varied the charge of C₂ atom on imidazolium ring from being essentially zero (−0.05e Mulliken population analysis) to positive (+0.26e natural population analysis), so it causes significantly different results even for the same sample.^{29,30} Nevertheless, some authors, for example Pádua and Borodin,^{31–34} have developed both the fixed charge and polarizable force fields for a series of imidazolium-based ILs, and the force field parameters were transferable between different combinations of cation/anion and validated against available solid- and liquid-state properties. However, the extension of the present force fields to other IL families would require the calculation of new intramolecular and charge distribution parameters by ab initio calculation. Therefore, the investigations based on electronic level provide more direct understanding about the intra- and intermolecular interactions of the molecules or ions, besides some thermodynamic properties. The charge distribution, the frontier orbitals, and the interactive energy become very important in finding the main decisive forces for the properties of ILs. Many ab initio DFT calculations^{35–37} and ab initio molecular dynamics³⁸ have been performed to investigate the structures and interactions, which show that the H-bonds and the local H-bonded network are the essential structural features for the behavior of ILs.

Despite the above-mentioned, there are still relatively few elaborate calculations at the electronic level about the ion pair, even ion clusters that may be directly composed of the elemental structural units in ILs. Moreover, most of the calculations only focused on the simple imidazolium-based halide ion pair (for example, [Dmim]Cl ion pair) with the single atomic anion.^{36–39} The complex fluoro-anion ILs ([Dmim][BF₄] and [Dmim][PF₆]) with multiple atomic anions have not reported. However, these fluoro-anion ILs are very promising in industrial applications because of their stability in the atmosphere. Therefore, in this work, we combined ab initio DFT calculations with experimental FTIR spectra to explore elaborately the geometric and electronic structures of [Emim][BF₄] and [Bmim][PF₆], whose aim is to provide the key evidence for the interionic interactions. Also some new methods provided by Gaussian09 version were used to compare the differences with the single atomic anion ILs (for example, [Emim][Cl]).

COMPUTATIONAL METHODS

All calculations were performed with the Gaussian09 B.01 version.⁴⁰ The structural optimizations were performed at the popular B3LYP/6-31++G(d,p) theoretical level. In the optimizing process, cations and ion pairs relaxed the symmetry constraint, while anions were considered the structural symmetry. All of the obtained geometries were confirmed by frequency to ensure no imaginary frequencies. In these calculations, the 6-31++G(d,p) basis set was stressed because it is of double- ξ quality for valence electrons with the certain consideration of diffuse functions. The initial configurations of the ion pairs were mainly based on the charge distribution and electrostatic potential on the isolated cation and anion. Thus, there are five favored positions in Figure 1 for the [BF₄][−] anion around the imidazolium cation. They are ethyl-front (anion locates in front of ethyl chain), ethyl-back (anion locates at

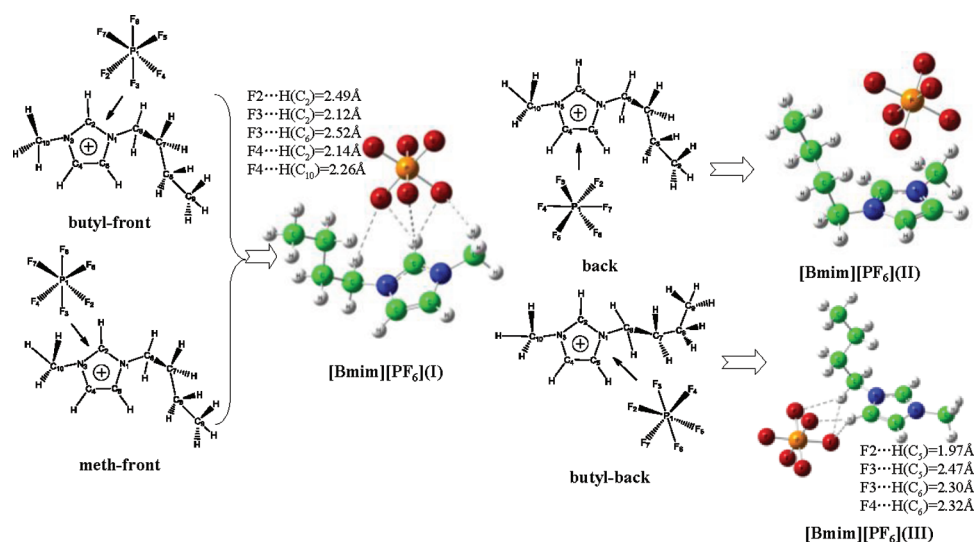


Figure 2. Optimized structures of the $[\text{Bmim}][\text{PF}_6]$ ion pair when the anion is located at possible five different positions around cation. The arrows represent the initial locations of the anion. The dashed lines noted the H-bonds in the ion pairs. C atoms (green), N atoms (blue), H atoms (gray), F atoms (brown), and P atoms (yellow) are shown in different colors for clarity.

the back of the ethyl chain), back (anion locates at the back of the cation), meth-back (anion locates at the back of the methyl chain), and meth-front (anion locates in front of the methyl chain). Very similar initial configurations of the $[\text{Bmim}][\text{PF}_6]$ ion pair are shown in Figure 2.

The interaction energies calculated at MP2/6-31++G(d,p) and B2PLYPD/6-31++G(d,p) theoretical levels were compared with the results of B3LYP/6-31++G(d,p). Emphatically, the B2PLYP is a new empirical hybrid functional with correction from perturbation theory, which is very successful in calculating the thermodynamic data yielding the smallest mean absolute deviation in many reported cases.⁴¹ However, a basic deficiency of this functional is correction with respect to the dispersion (VDW) interaction. In B2PLYPD, the D term was added empirically and represents the dispersion correction. The total energy could be written as the following equation:

$$E_{\text{DFT-D}} = E_{\text{KS}} + E_{\text{disp}},$$

$$E_{\text{disp}} = -s_6 \sum_{i=1}^{N_{\text{at}}-1} \sum_{j=i+1}^{N_{\text{at}}} \frac{C_6^{ij}}{R_{ij}^6} f_{\text{dmp}}(R_{ij}) \quad (1)$$

Here, N_{at} is the number of atoms in the system, C_6^{ij} denotes the dispersion coefficient for atom pair ij , s_6 is a global scaling factor that only depends on the functional used and R_{ij} is the interatomic distance.⁴¹ Natural population analysis (NPA) and natural bond orbital (NBO) analysis of the conformers were carried out using version 3 of Gaussian09.^{42,43} Symmetry-adapted perturbation theory (SAPT) was designed to calculate the interaction energy of a dimer. In SAPT, the interaction energy is expressed as a sum of perturbative corrections, each correction resulting from a different physical effect. This decomposition of the interaction energy into distinct physical components is a unique feature of SAPT which distinguishes this method from the popular supermolecular approach.⁴⁴

EXPERIMENTAL SECTION

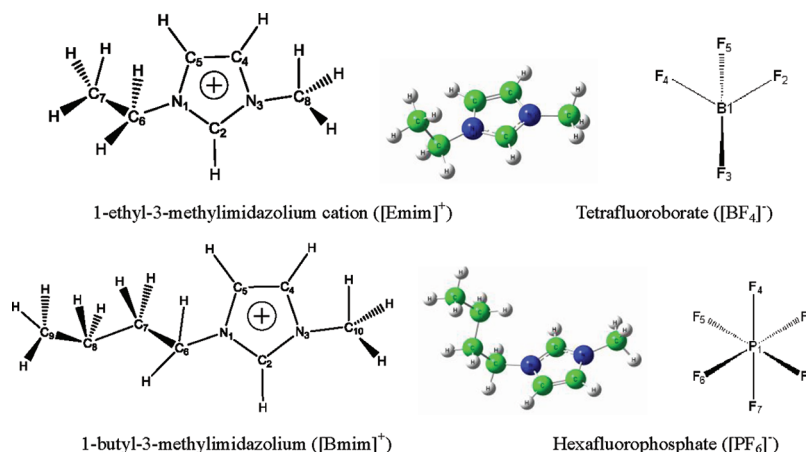
$[\text{Bmim}][\text{PF}_6]$ was synthesized in two steps in our laboratory. Equal molar amounts of 1-chlorobutane and *N*-methylimidazole were added to a flask fitted with a reflux condenser for 72 h at

343 K with stirring until two layers formed. The top layer was decanted and ethyl acetate was added with thorough mixing. The ethyl acetate was decanted and fresh ethyl acetate was added. This step was repeated twice. After the third decanting of ethyl acetate, $[\text{Bmim}][\text{Cl}]$ was obtained after being dried in vacuum oven at 343 K for 48 h. $[\text{Bmim}][\text{Cl}]$ was transferred to a plastic container followed by addition of deionized water. An aqueous solution of 60% HPF_6 (HBF_4) with 1.1:1 molar ratio was added. After HPF_6 was added, two phases formed, where $[\text{Bmim}][\text{PF}_6]$ was obtained at the bottom phase. Then the products were dried at 343 K on a vacuum line for 4 h. The water content was then determined by Karl Fisher titration and was found to be below 300 ppm. FT-IR measurement was performed with Thermo Nicolet Magna-IR 750 spectrometer at 298.15 K and 1 atm. The accessible spectral regions are mid-IR of 400–4000 cm^{-1} and far-IR of 50–650 cm^{-1} using a KBr window. $[\text{Emim}][\text{BF}_4]$ was obtained via the similar procedure.

RESULTS AND DISCUSSION

1. Structures of Isolated Cation and Anion. The labeled structures of the isolated cation and anion are shown in Scheme 1. The most stable geometries are identified from the lowest-energy conformers. Two anions possess highly geometric symmetries, ($[\text{BF}_4]^-$ T_d , $[\text{PF}_6]^-$ O_h). However, the symmetries of the two cations were not restricted. The C_1 conformer of $[\text{Emim}]^+$ cation was obtained and is shown in Scheme 1 in the ball–stick fashion. Due to the long and flexible butyl chain, $[\text{Bmim}]^+$ cation has the nine possible conformers. The lowest-energy conformer with the zigzag butyl chain is also shown in Scheme 1 in the ball–stick fashion. The frequencies were calculated after optimizing all of the conformers, and no imaginary frequencies could be found.

Although connecting with different alkyl chains, the features of electronic structures for $[\text{Bmim}]^+$ and $[\text{Emim}]^+$ are similar to each other. The ring is aromatic (four electrons on two N atoms and two electrons on three C atoms) and $6p_\pi$ electrons shared the $5p_\pi$ orbitals, and the electrons are fully delocalized on it. NBO analysis also shows that the double bond between C_4 and C_5 atoms and the other four electrons are delocalized around the

Scheme 1. Structures of the Isolated [Emim]⁺ and [Bmim]⁺ Cations, and [BF₄][−] and [PF₆][−] Anions^a

^a The most stable conformers for the two cations are shown in ball and stick fashion at the B3LYP/6-31++G** level, respectively, in which C atoms are green, N atoms are blue, and H atoms are gray.

N₁–C₂–N₃ group. The acidity of the three H atoms on ring and its influence on the properties of ILs are still controversies. Based on our calculations, the larger positive charges at C₂–H group indicate the more acidic than C_{4/5}–H groups by NPA.

2. Structures of Isolated Ion Pairs. The properties of the solutions are always determined by the intermolecular interactions. RTILs are composed of ions completely so that the ion pairs as the basic structural units are very important in exploring ILs.⁴⁵

Based on the NBO charges on [Emim]⁺ cation, there are five possible positions in which the [BF₄][−] anion locates around cation as the ethyl-front, meth-back, back, meth-front, and ethyl-back marked by arrows in Figure 1. The five initial configurations were optimized at the B3LYP/6-31++G** level. Finally, three lowest-energy conformers were obtained and are shown in the ball–stick fashion in Figure 1. [Emim][BF₄](I) was obtained from the ethyl-front, meth-back, and back configurations. The [BF₄][−] anion moved to the upper part of ring from the lateral part and locates near C₂–H group. The [Emim][BF₄](II) was obtained from the meth-front, in which the [BF₄][−] anion also moves to the upper part of ring. The [Emim][BF₄](III) was obtained from the ethyl-back, in which the [BF₄][−] anion only locates near the C₅–H group.

A shallow potential energetic well was obtained when the [BF₄][−] anion locates at the back position of the imidazolium cation and experiences minimal electrostatic attraction to the significantly stronger electrostatic attraction due to the positive C₂ atom and the essentially neutral C_{4/5} atoms. While localizing at the ethyl-back position, it is very difficult for the [BF₄][−] anion to move largely due to steric exclusion from ethyl side chain and the repulsion from π electrons between C₄ and C₅ atoms.

As the intermolecular interactions determine the properties of the substances, many experiments have confirmed that H-bonds play very important roles in some chemical and biological processes.^{46,47} For example, each water molecule is connected with neighbors by the strong H-bonds, and the phase behaviors occurring in water are closely related to the H-bonds.⁴⁸ Up to date, many researchers have also investigated the interactions in ILs and found that H-bonds are also the most explicit non-covalent interactions and play a very key role in the behaviors of ILs.^{13,20,24,35,49–52}

In common, a geometric criterion for a H-bond is the distance between the proton on the donor group and the acceptor atom, namely $R_{XH\cdots Y}$, which is less than the sum of their van der Waals radii; herein the van der Waals distance for F \cdots H is 2.670 Å.¹⁵ Thus, there are four F \cdots H H-bonds in the [Emim][BF₄](I) ion pair as shown by dashed lines in Figure 1. Two H-bonds are between the F atoms (labeled as F₂) and H(C₂) atom of the ring and H(C₆) atom of the alkyl chain. The distances are 2.02 and 2.54 Å, respectively. The other two occur between the F₃ atom and the H(C₂) atom and the H(C₈) atom of alkyl chain. The distances are 2.29 and 2.21 Å, respectively. A similar structure can be seen in the [Emim][BF₄](II) ion pair, except that there is no H-bond between the F₃ atom and H(C₂) atom. In [Emim][BF₄](III) ion pair, the [BF₄][−] anion locates at the ethyl back of the cation as the ethyl-back conformer shown in Figure 1; there are three H-bonds, and they are between the F₂ atom and H(C₂) atom of ring, between the F₃ atom and H(C₆) atom of alkyl chain, and between the F₄ atom and H(C₇) atom of alkyl chain. Their distances are 1.91, 2.05, and 2.40 Å, respectively.

For [Bmim][PF₆] ion pair, the five initial configurations, including butyl-front, meth-back, back, meth-front, and butyl-back, were optimized at the B3LYP/6-31++G** level completely. Also, the three lowest energy conformers were obtained (see Figure 2). The [Bmim][PF₆](I) ion pair was obtained from the butyl-front and the meth-front. [Bmim][PF₆](II) and [Bmim][PF₆](III) ion pairs were obtained from the back and the butyl-back, respectively. However, no stable point was found at the potential energy surface for the meth-back initial configuration either at the MP2 or DFT theoretical level. For the back conformer, the [PF₆][−] anion moves above the imidazolium ring and the steric exclusion of the long butyl chain leads to the conformer.

There are five H-bonds in [Bmim][PF₆](I) ion pair as drawn by dashed lines in Figure 2. One is between the F₂ atom of [PF₆][−] anion and H(C₂) atom of imidazolium ring with the distance of 2.49 Å. Two are between the F₃ atoms and H(C₂) atom, and H(C₆) atom of alkyl chain. The distances are 2.12 and 2.52 Å, respectively. The other two are between the F₄ and H(C₂) atom, and H(C₁₀) atom of alkyl chain, and the distances are 2.14 and 2.26 Å, respectively. There are four H-bonds in [Bmim][PF₆](III). One is between the F₂ atom and H(C₅) of

Table 1. Interaction Energies (kJ/mol) of [Emim][BF₄] Ion Pairs Calculated at the Different Theoretical Levels

| | B3LYP | B2PLYP | MP2 | B2PLYPD | $E_{n_F \rightarrow \sigma_{C-H}^*}^{2a}$ |
|-------------------------------|--------|--------|--------|---------|---|
| [Emim][BF ₄](I) | 348.14 | 354.44 | 371.77 | 372.03 | 55.90 (32.84,59%) |
| [Emim][BF ₄](II) | 348.14 | 353.39 | 361.27 | 369.93 | 54.68 (31.67, 58%) |
| [Emim][BF ₄](III) | 314.54 | 319.26 | 325.82 | 330.91 | 84.18 (48.32,57%) |

^aThe second-order perturbation energies for the H-bond from NBO analysis, and the data in parentheses are the energies and percentage of interaction between [BF₄][−] anion and C—H of imidazolium ring, $n_F \rightarrow \sigma_{C-H}^*$.

Table 2. Interaction Energies (kJ/mol) of [Bmim][PF₆] Ion Pairs Calculated at the Different Theoretical Levels

| | B3LYP | B2PLYP | MP2 | B2PLYPD | $E_{n_F \rightarrow \sigma_{C-H}^*}^{2a}$ |
|-------------------------------|--------|--------|--------|---------|---|
| [Bmim][PF ₆](I) | 319.00 | 331.86 | 340.79 | 346.57 | 55.35(37.53,68%) |
| [Bmim][PF ₆](II) | 306.66 | 321.36 | 330.50 | 343.68 | — |
| [Bmim][PF ₆](III) | 289.07 | 298.52 | 309.28 | 311.38 | 59.79(40.29,67%) |

^aThe second-order perturbation energies for the H-bond from NBO analysis, and the data in parentheses are the energies and percentage of interaction between [PF₆][−] anion and C—H of imidazolium ring, $n_F \rightarrow \sigma_{C-H}^*$.

the ring, and the distance is 1.97 Å. The other three are between two F atoms and H(C₅) and H(C₆) of alkyl chain, and the distances are 2.47, 2.30, and 2.32 Å, respectively. However, when the [PF₆][−] anion locates at the back of the imidazolium ring, the [PF₆][−] anion moves above the imidazolium ring to form [Bmim][PF₆](II) and there is no H-bond forming.

Obviously, although the number and fashion are very different, the H-bonds are the explicit structural features in the two typical ion pairs. Moreover, the feature of more than one H-bond between cation and anion is different from the ILs with a single atomic anion, like dialkylimidazolium chloride ([Emim][Cl]), in which there is only one H-bond between the cation and anion.^{35,36}

3. Interaction Energies of Ion Pairs. The interaction energy is often seen as one of the most important structural parameters to correlate with the properties of RTILs. The interaction energy is usually defined as the energetic difference between dimer (or an ion pair) and two monomers (or a cation and anion). Tables 1 and 2 list the interaction energies of these optimized [Emim][BF₄] and [Bmim][PF₆] ion pairs at the different theoretical levels using the same 6-31++G** basis set, in which the diffuse functions were added to heavy atoms (d orbital functions) and H atoms (p orbital functions) to consider the long-range interactions. It has been confirmed that the choice of the basis set cannot largely improve the interaction energies because the major source of interaction is the charge–charge attraction.⁵³ As a rule, the MP2 is more reliable to estimate the interaction energy than DFT energy due to the DFT's defective consideration for the dispersion force.

From the data in Table 1, it can be seen that MP2 energies are 20–30 kJ/mol larger than DFT energies that may represent the missing long-range interaction from DFT methods.⁵⁴ B2PLYP developed by Grimme et al. is a new semiempirical hybrid functional with perturbation correction recently.⁵⁵ The B2PLYP energies are comparative with B3LYP with about 5 kJ/mol differences in the three [Emim][BF₄] ion pairs. However, the B2PLYP+D significantly improves the energetic estimation after dispersion correction (D term is an empirical correction for the long-range dispersion), which are very comparative with MP2

energies.⁴¹ For example, the B2PLYP energy of [Emim][BF₄](III) is 332.91 kJ/mol, which is 7 kJ/mol larger than the MP2 energy. And for [Emim][BF₄](I), B2PLYP energy is 372.03 kJ/mol and the difference is only 0.26 kJ/mol with MP2. Moreover, the D term provides a quantitative evaluation for the possible defective dispersion interaction between cation and anion. From Table 1, the differences between B2PLYP and B2PLYPD are 17.59, 16.54, and 11.62 kJ/mol for the three ion pairs, respectively. The dispersion interaction of [Emim][BF₄] IL is less than 5% of total energy in the equilibrium distance which is very similar to the results from the symmetry-adapted perturbation theory (SAPT) evaluation.⁵⁶

Compared to the three [Emim][BF₄] ion pairs, all of the interaction energies of [Bmim][PF₆] in Table 2 ion pairs decreased correspondingly, but the energetic estimations based on the different methods are very similar to the ones in Table 1. Likewise, MP2 and B2PLYPD are more accurate than the DFT theory. The D term gives an estimation of the dispersion interaction with less than 5% of total energy.

Generally, all of the interaction energies in these ion pairs are larger than 300 kJ/mol, even are 10 orders of magnitude of water (~23 kJ/mol) due to the strong electrostatic attraction between cation and anion. However, many researchers have inferred that other forces besides pure Coulombic force also play an important role on the properties of ILs.^{36,56} Thus, we employed SAPT to decompose the total interaction energy of [Emim][BF₄](I) into different parts in analogy to a multipole expansion in order to explore the different contributions. In SAPT, the interaction energy can be computed at different levels of intramonomer correlations, which provide an accurate description of intermolecular interactions and compensate for the deficiency of HF theory, especially for the exchange energy and van der Waals interaction.

The obtained total SAPT energy for [Emim][BF₄](I) ion pair is 333.38 kJ/mol, in which the electrostatic attraction (91.59 kJ/mol) is 71% of the total interaction energy, the exchange energy (18.56 kJ/mol) is 14.4%, the induction term (12.78 kJ/mol) is 10%, and the dispersion term (6.09 kJ/mol) is 4.7%. Though the electrostatic attraction is the main contribution to the total energy, ILs are not the same as the typical high-temperature molten salts (NaCl) as one imagines intuitively. For ILs, the other forces are not negligible, and the different contributions compensate each other partly so as to result in the unique properties.

On the other hand, the general $n_Y \rightarrow \sigma_{X-H}^*$ donor–acceptor H-bonded interaction ($XH \cdots Y$) can be evaluated by the perturbation theory to calculate the delocalization energies, E^2 as follows

$$E^2 = \Delta E_{ij} = q_i \frac{(F_{i,j})^2}{e_i - e_j} \quad (2)$$

where q_i is the donor orbital occupancy, e_i and e_j are diagonal elements (orbital energies), and $F_{i,j}$ is the off-diagonal NBO Fock matrix element.

In Tables 1 and 2, the E^2 energies obtained from NBO analysis represent the different capacities to form $n_F \rightarrow \sigma_{C-H}^*$ H-bonds for these ion pairs. The E^2 for [Emim][BF₄](I) and [Emim][BF₄](II) ion pairs are 55.90 and 54.68 kJ/mol, which exhibit the very similar H-bonded capacities. However, the E^2 of [Emim][BF₄](III) ion pair is 84.18 kJ/mol and the stronger capacity is shown. Obviously, this did not exhibit the consistent change with the previous total interaction energies and number of H-bonds.

Table 3. NPA Charges of the Isolated Cation and Anion, and [Emim][BF₄](I) and [Emim][BF₄](III) Ion Pairs

| | isolated ion | [Emim][BF ₄](I) | [Emim][BF ₄](III) |
|---------------------|---------------------|-----------------------------|-------------------------------|
| N1 | −0.346 | −0.356 | −0.337 |
| C2 | 0.268 | 0.308 | 0.246 |
| N3 | −0.348 | −0.355 | −0.361 |
| C4 | −0.038 | −0.056 | −0.071 |
| C5 | −0.035 | −0.054 | 0.000 |
| C6 | −0.249 | −0.247 | −0.262 |
| C7 | −0.680 | −0.681 | −0.676 |
| C8 | −0.449 | −0.454 | −0.445 |
| H(C2) | 0.269 | 0.302 | 0.252 |
| H(C4) | 0.279 | 0.259 | 0.265 |
| H(C5) | 0.278 | 0.260 | 0.316 |
| H(C6), H(C6) | 0.256, 0.263 | 0.236, 0.278 | 0.309, 0.231 |
| H(C7), H(C7), H(C7) | 0.243, 0.244, 0.264 | 0.220, 0.245, 0.278 | 0.211, 0.251, 0.272 |
| H(C8), H(C8), H(C8) | 0.256, 0.262, 0.262 | 0.292, 0.242, 0.236 | 0.245, 0.250, 0.250 |
| Total | +1 | 0.953 | 0.946 |
| B1 | 1.435 | 1.432 | 1.430 |
| F2 | −0.609 | −0.566 | −0.595 |
| F3 | −0.609 | −0.608 | −0.600 |
| F4 | −0.609 | −0.607 | −0.611 |
| F5 | −0.609 | −0.604 | −0.570 |
| total | −1 | −0.953 | −0.946 |

Compared with the typical aprotic [Emim][Cl] ion pair ($E^2 = 161.75$ kJ/mol, at B3LYP/6-31++G** level) and the protic [PrAm][NO₃] ion pair ($E^2 = 250.49$ kJ/mol, at B3LYP/6-31+G* level),⁵¹ all of the studied ion pairs present the weaker H-bonded capacity. One reason is that [Cl][−] anion possesses a stronger Lewis base than [BF₄][−] and [PF₆][−] anions that results in a larger delocalization correction to the zeroth-order natural Lewis structure. But in the protic ILs, the possible proton transfer can restore the ions to the acid and base molecules by H-bonds to obtain the largest delocalization correction. However, compared with the molecular solvent system, such as F₃CH/H₂O system⁵⁷ ($E^2 = 27.36$ kJ/mol), the obtained ion pairs present strong H-bonded capacities. It indicates that the strength of H-bonded interaction is greatly enhanced if the Lewis base is an anion and the Lewis acid is a cation. Moreover, it was found that the interaction mainly derives from the $n_F \rightarrow \sigma_{C-H}^*$ delocalization between [BF₄][−] anion and C–H groups of the imidazolium ring. These energies are more than 50% of the total delocalization energies for the three ion pairs (Table 1), which indicates the cooperative interaction between the electrostatic attraction and H-bonds.

From Table 2, it can be seen that [Bmim][PF₆](I) and [Bmim][PF₆](III) ion pairs exhibit weaker H-bonded capacities than the corresponding [Emim][BF₄] ion pairs. However, the interactions from the $n_F \rightarrow \sigma_{C-H}^*$ delocalization are more remarkable than from [Emim][BF₄] ion pairs and the energies are more than 60% of the total delocalization energies. For [Bmim][PF₆](II), when [PF₆][−] anions moved above the imidazolium ring, there were no Lewis electrons transfer so that the delocalization of the $n_F \rightarrow \sigma_{C-H}^*$ H-bond was not observed by NBO analysis.

4. Charge Distribution. The charge distribution on each atom is responsible for the local electrostatic potential and decides the interactions between ions. The NPA charges of both isolated [Emim]⁺ and [BF₄][−] ions and [Emim][BF₄] ion pairs are listed

in Table 3. Additionally, [Emim][BF₄](II) has almost the same NPA charges as [Emim][BF₄](I), so they are not listed in Table 3.

For the isolated [Emim]⁺ cation in Table 3, three H atoms on the ring are distributed by the largest positive charges, and the C₂ atom is also with significant positive charges. But two N atoms are distributed by negative charges and C₄ and C₅ atoms are near neutral. Although the positive charges on three H atoms are nearly the same, it does not mean that there are the same Lewis acidities. The charges with H atoms summed into heavy atoms are $q(C_2) = 0.382$, $q(C_4) = 0.153$, $q(C_5) = 0.154$ at B3LYP/6-31++G** theory level, which indicates that the relative acidity should be associated with C–H groups. NPA analysis also showed that the C atoms on the alkyl chain are distributed by the negative charges and the H atoms by significant positive charges, while C–H groups are neutral essentially, which indicates that the interaction derived from the alkyl chains is mainly van der Waals interaction rather than Coulombic force. For the isolated anion, the four F atoms are distributed by the same negative charges and the B atom is with the large positive charge.

In the [Emim][BF₄](I) ion pair compared with the isolated cation, no significant change is found for the charge on the two N atoms of the imidazolium ring. However, the positive charge on H(C₂) atom increases from 0.269 to 0.302 and on C₂ atom decreases from 0.268 to 0.308. Correspondingly, the positive charge on the H(C₄) atom decreases from 0.279 to 0.259 and decreases from 0.278 to 0.260 on H(C₅), and no significant changes are found for C₄ and C₅ atoms. It indicates that the partial π electrons transfer along the ring from C₂–H group to the back-side H(C₄) and H(C₅) atoms due to the repulsion between anion electrons and the π electrons on ring. Figure 3A shows the direction of the transfer, and finally the C₂–H group (noted by the red color in Figure 3A) is distributed by the largest positive charges. The charges on alkyl chains have no significant changes except that the small changes are induced by van der

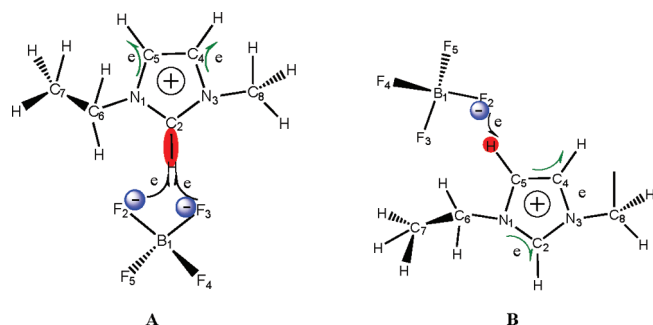


Figure 3. Direction of charge transfer when the anion approaches the cation.

Waals interaction on H atoms that connect with anion. For anion, the charges on the four F atoms increase a little, and the most remarkable change occurs on the F₂ atom which is near to the C₂–H group and the charge increases from -0.609 to -0.566 . Finally, the total positive charge on cation decreases from 1 to 0.953 and the total negative charge on anion increases from -1 to -0.953 , while a small charge transfer of 0.047 occurs from anion to cation.

When the anion locates at the back of cation as in the [Emim][BF₄](III) ion pair, two N atoms have no significant charge changes and both C₄ and C₅ atoms remain neutral. However, the charge on H(C₅) increases from 0.278 to 0.316 (noted by red color in Figure 3B), and the positive charge on H(C₄) also increases significantly. Correspondingly, the positive charge on both C₂ and H(C₂) atoms decrease. Finally, the total positive charge on cation decreases from 1 to 0.945 and the total negative charge on anion increases from -1 to -0.945 , and a small charge transfer of 0.054 also occurs from anion to cation. The electrostatic repulsion between the anion and the delocalized π electrons of ring is responsible for a partial electron transfer as shown in Figure 3B.

The same trend of the charge transfer can be found in [Bmim][PF₆](I) and [Bmim][PF₆](III) ion pairs. But in the [Bmim][PF₆](II) ion pair, the anion moves above the imidazolium ring and the strong electrostatic repulsion between anion and the delocalized π electrons on ring results in the significant decrease of the positive charges on three H atoms and the increase of the positive charge on C₂ atom of ring.

5. Orbital Analysis of H-Bonds. Compared with the [Emim]⁺ cation, it was found in [Emim][BF₄] ion pairs that the occupation on N₃ orbital always increases, while the occupations on $\pi_{C2=N1}$ and $\pi_{C4=C5}$ orbitals vary with the positions of anion by NBO analysis. In [Emim][BF₄](I) and [Emim][BF₄](II) ion pairs, the occupation on the $\pi_{C2=N1}$ orbital decreases, but on the $\pi_{C4=C5}$ orbital it increases. In the [Emim][BF₄](III) ion pair, the occupation of the $\pi_{C4=C5}$ orbital decreases, and the occupation on the $\pi_{C2=N1}$ orbital exhibits no significant change. Obviously, the electron repulsion between p electrons of [BF₄][−] anion and the π electrons of ring is responsible for the charge occupation.

Furthermore, the canonical molecular orbital analysis provides us an essential understanding for the charges transfer and H-bonded interaction. Figure 4 shows these frontier molecular orbitals (FMOs) energy-order diagram for both [Emim][BF₄](I) and [Emim][BF₄](III) ion pairs. The HOMO of the isolated anion is three degradation p orbitals (the orbital energy $E = -0.256$ in Figure 4) and the LUMO of the isolated cation is the anti- π (π^*) bond orbital (the orbital energy $E = -0.189$) with four energetic

nodes. When the anion approaches the cation to form the ion pair, there is not the expected p– π orbital overlap, but the HOMO of the [Emim][BF₄](I) ion pair composed of the highest occupied p orbital of anion and the lowest empty $\pi^*_{(C2-H)}$ orbital of cation exhibits a covalent characteristic σ – σ overlap. Meanwhile, the π electrons are significantly polarized along with the C₂–H bond. The LUMO of [Emim][BF₄](I) exhibits an anti- σ (σ^*) bond orbital (the orbital energy $E = -0.0522$). In [Emim][BF₄](III) ion pair, the effective orbital overlap also occurs and the ion pair HOMO (the orbital energy $E = -0.304$) and the degradation HOMO-1 (the orbital energy $E = -0.302$) composed of the highest occupied p orbital of anion and the lowest empty $\sigma^*_{(C5-H)}$ and $\sigma^*_{(C6-H)}$ orbital of cation also exhibit the σ -type orbital overlap, but the π electrons are not significantly polarized along with the C₅–H and C₆–H bonds, respectively. Likewise, the LUMO of the ion pair is the σ^* bond orbital (the orbital energy $E = -0.0765$). Figure S1 in the Supporting Information shows the possible positions of H-bonded interactions in [Emim][BF₄](I) and [Emim][BF₄](III) ion pairs obtained by RDG function (reduced density gradient).

The σ -type interaction rather than p– π overlap embodies a moderate covalent bonding feature. But the formation of the covalent H-bonds must require a stronger intermolecular attraction. The electrostatic attraction drives the anion to approach the cation, and finally locates at the largest positive charge position of cation. After forming ion pair, although the repulsion of the electron between anion and cation increases the total energy, the orbital effective overlap and the partial electrons transfer between anion and cation result in a more significant reduction of the total energy, and further stabilize the ion pairs. However, it can be seen in Figure 4 that the anion still is dominative in the ion pair HOMO and is expected to favor accepting H-bonds, but it will not release significantly more charge. The ion pair LUMO is the antibonding orbital and electron acceptance is not favorable. That is why only H-bonds rather than covalent bonds can form between anion and cation. This analysis of the electronic structure provides us some key evidence to understand the nature of interactions in ILs.

Table 4 also lists the electron densities and the total electrostatic potentials (ESP) for both isolated [BF₄][−] and [PF₆][−] anions at different sites centered by B atom and P atom, respectively. The electron densities of [BF₄][−] anion are always larger than that of [PF₆][−] anion at all of sites though the ESP is very similar for the two species. This also indicates that the interaction energies of [Emim][BF₄] ion pairs are always larger than those of [Bmim][PF₆] ion pairs at different theoretical levels.

6. Ion Clusters and Local H-Bonded Network. As reported,^{58–60} the ion cluster by multiple ions connected with each other can reflect the arrangement of ions in the bulk phase of RTILs.⁶¹ These ion clusters may become microscopic models to describe the structures of the bulk ionic liquids or their aqueous solutions. Figure 5 shows an experimental FTIR spectrum of [Emim][BF₄] IL and the calculated IR vibrational frequencies for the ([Emim][BF₄])_n ion clusters with different numbers, $n = 2, 3, 4$, and 5, at the B3LYP/6-31+G** theoretical level. The strong agreement on the major bands provided the possibility to explore the detailed structural information of [Emim][BF₄] IL, and these experimental vibrations can also be assigned rationally by the structures of these ion clusters.

Three main bands were labeled in the experimental IR (red solid line in Figure 5). The first band occurs at 3000–3500 cm^{−1} and is assigned to the symmetric stretches of three C–H bonds on the imidazolium rings, and the strongest peaks are the

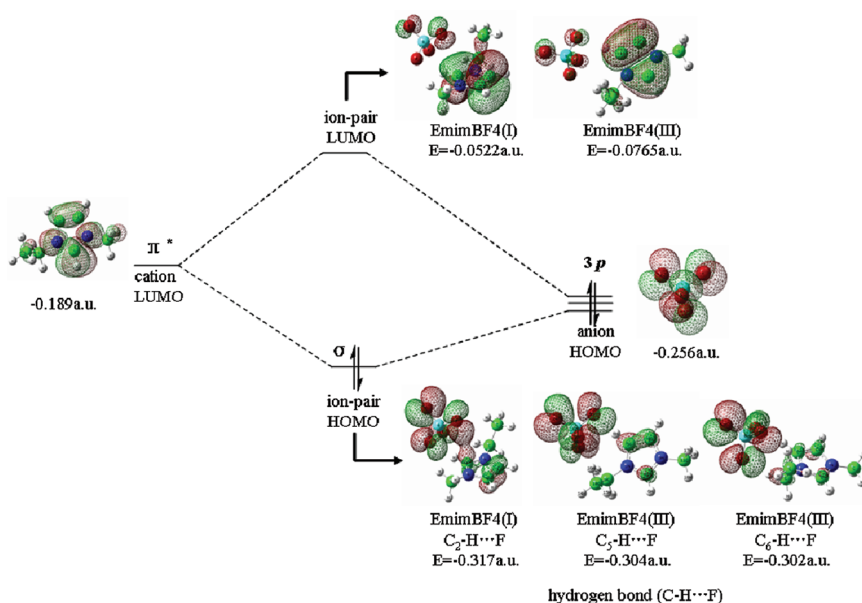


Figure 4. Energy diagram of $[\text{Emim}][\text{BF}_4](\text{I})$ and $[\text{Emim}][\text{BF}_4](\text{III})$ ion pairs when the $[\text{BF}_4]^-$ anion approaches $[\text{Emim}]^+$ cation to form the stable ion pairs. (Due to being the same orbital diagram with the $[\text{Emim}][\text{BF}_4](\text{I})$, the $[\text{Emim}][\text{BF}_4](\text{II})$ ion pair is not drawn. The a. u. is the energy atomic unit (Hartree).)

Table 4. Electron Densities and EPS of $[\text{BF}_4]^-$ Anion and $[\text{PF}_6]^-$ Anion at Different Positions^a

| | 1.8 Å | 2.0 Å | 2.2 Å | 2.4 Å | 2.6 Å | 2.8 Å | 3.0 Å |
|--|-----------------------|----------------------|-----------------------|-----------------------|-----------------------|-----------------------|-----------------------|
| electron density ($[\text{BF}_4]^-$) | 1.06×10^{-4} | 3.9×10^{-5} | 1.45×10^{-5} | 5.13×10^{-6} | 1.81×10^{-6} | 6.80×10^{-7} | 2.77×10^{-7} |
| EPS($[\text{BF}_4]^-$) | 0.163 | -0.149 | -0.136 | -0.125 | -0.116 | -0.108 | -0.101 |
| electron density ($[\text{PF}_6]^-$) | 0.8×10^{-5} | 2.9×10^{-5} | 1.04×10^{-5} | 3.65×10^{-6} | 1.35×10^{-6} | 5.41×10^{-7} | 2.28×10^{-7} |
| EPS($[\text{PF}_6]^-$) | -0.159 | -0.146 | -0.135 | -0.125 | -0.116 | -0.108 | -0.101 |

^a Two distributions are centered by B atom for BF_4^- anion and P atom for PF_4^- anion, respectively.

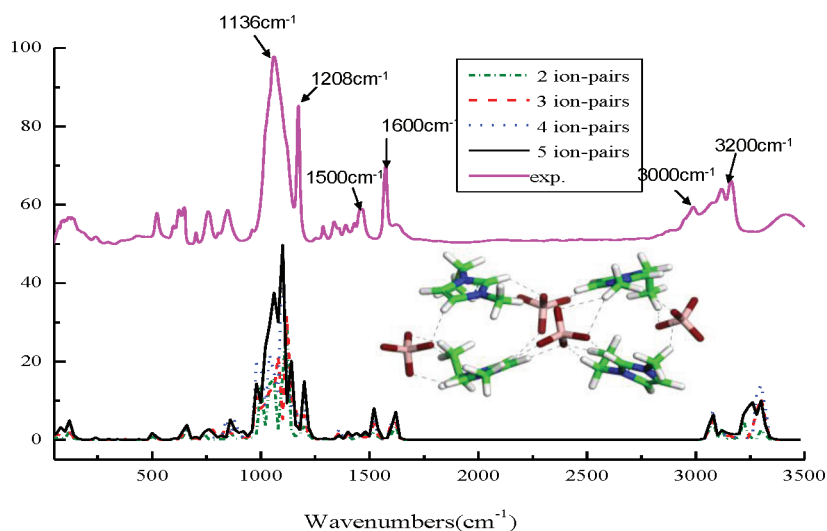


Figure 5. Measured FTIR spectrum of $[\text{Emim}][\text{BF}_4]$ at room temperature condition compared to the vibrational modes of the corresponding ion clusters $([\text{Emim}][\text{BF}_4])_n$ with $n = 2, 3, 4$, and 5 calculated by DFT at the B3LYP/6-31+G** level (all of the calculated bands were corrected by the factor 0.964–0.967). The local H-bonded network with four ion pairs is also showed in tube style.

stretches of $\text{C}_2\text{--H}$ bonds. Two weaker bands around 1600 and 1500 cm^{-1} can be assigned to the breaths of the rings and the scissors of the alkyl chains, respectively. The peaks around 1208 cm^{-1} are assigned to the interplanar wagging vibrations of

the C--H bonds on rings. The strongest peak around 1136 cm^{-1} is assigned to the stretches of B--F bonds of $[\text{BF}_4]^-$ anion in various directions, while these weak peaks around 750–880 cm^{-1} are the out-of-planar wagging vibrations of the rings. Though the ion

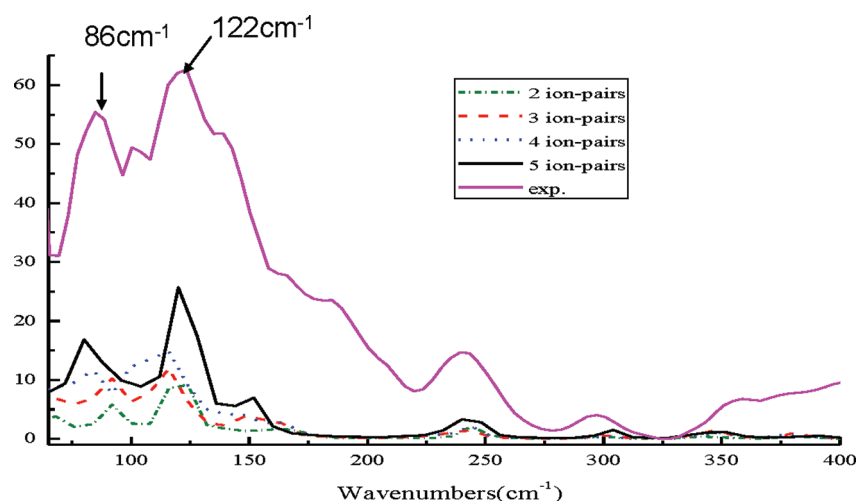


Figure 6. Measured far-IR region of 50–400 cm^{-1} of $[\text{Emim}][\text{BF}_4]$ at room temperature compared to the vibrational modes of the corresponding clusters $([\text{Emim}][\text{BF}_4])_n$ with $n = 2, 3, 4$, and 5 calculated by DFT at the B3LYP/6-31+G** level (all calculated bands were corrected by the factor 0.964–0.967).

clusters with different number present the typical gas structures, they reproduce the vibrational modes of experimental result, and thus it indicates that these cluster structures can lead to insight into the bulk phase of ILs.

Recent studies have found that the H-bonded network structure of water was measured by the IR spectra of precisely size selected, protonated water clusters $\text{H}^+(\text{H}_2\text{O})_n$ up to $n = 200$.⁶¹ As discussed above, H-bonds are also the important interionic interactions to connect these discrete ions in ILs. Ludwig et al. studied the structural characteristics of H-bonds and found the ions can form quasi-3D H-bonded network structure in some ILs.^{21,62} In Figure 6 we present the experimental and calculated far-IR spectra for characteristic of ion–ion stretching and bending vibrational bands involving in H-bonds in $[\text{Emim}][\text{BF}_4]$ IL. The experimental bands can be reproduced by the calculated and deconvoluted vibrational bands. The very weak bands above 250 cm^{-1} are assigned to the bending and torsional modes of cations. The calculated frequencies of the ion clusters suggest that the stronger bands around 122 cm^{-1} can be attributed to the asymmetric and symmetric stretching modes of the $\text{CH}\cdots\text{F}$ hydrogen bonds. The bands around 86 cm^{-1} can be assigned to corresponding bending modes of these H-bonds.

The structural investigation into these clusters has implied that the ion arrangements are ordered and similar to the crystal structure of X-ray $[\text{Emim}][\text{BF}_4]$.^{63,64} The calculated ion clusters are shown in Figure S2 of the Supporting Information, and Figure 5 only shows one of ion clusters with $n = 4$. It is found that these ions are connected by the H-bonds (dashed lines) to form 3-dimensional H-bonded network as discussed in our previous studies.³⁵

In these networks, the ion stacks are influenced very little by the intramolecular bonding structures and the number of ion pairs, and the imidazolium cations are arranged by the alternative layers and the $[\text{BF}_4]^-$ anions are sandwiched between two cations, but do not locate above the rings and prefer to locate near the C–H groups of rings in these clusters. The cation–cation distance is around 5.10 Å between H(C_2) atom and the imidazolium ring center. No strong interaction between the ring proton and π -electron cloud of the imidazolium ring is observed and the ethyl groups stick out of the imidazolium ring planes

($\text{C}_2\text{--N}_1\text{--C}_6\text{--C}_7$ torsion angle around 74°). $[\text{BF}_4]^-$ anions form a pillar with a $\text{B}\cdots\text{B}$ 5.7 Å distance in two different anions. Neutron diffraction studies on some RTILs indicated that charge ordering endured in the liquid phase. In the $[\text{Mmim}][\text{Cl}]$ and $[\text{Mmim}][\text{BF}_4]$ salts, the molecular stacking in the first two or three solvation shells are similar to the crystal structures, although the atomic distances are altered in the liquid.^{65,66} MD simulations for the bulk $[\text{Emim}][\text{BF}_4]$ further confirmed the similar ion arrangement in bulk liquid phase by center of mass radial distribution function (RDF). The strong peak of RDF for cation–cation is about 5.0 Å and for anion–anion is about 5.6 Å which are consistent with the calculated distances in this work. Moreover, spatial distribution functions (SDFs) calculated by MD also found that the anion prefers the positions close to the H atoms of imidazolium ring and the H-bonded structure can extended into 3-dimensions.^{50,67,68}

In general, the ions in bulk phase are not randomly stacked and the electrostatic force, van der Waals and H-bonds rationalize the preferable arrangement. Furthermore, H-bonds are still most apparent interactions between cations and anions and form local quasi-3-dimensional (quasi-3D) network structures as shown in Figure S2 by the dashed lines. The experiments have confirmed that the local quasi-3D network of H-bonds is responsible for some properties of the bulk ILs, such as melting points and viscosities.^{19,21,62}

CONCLUSION

The electronic structures, especially the H-bonds of the two typical air-stable ILs ($[\text{Emim}][\text{BF}_4]$ and $[\text{Bmim}][\text{PF}_6]$), were investigated by DFT calculations. Three lowest-energy conformers were obtained from five initial configurations for both $[\text{Emim}][\text{BF}_4]$ and $[\text{Bmim}][\text{PF}_6]$ ion pairs, respectively. Anion prefers to be close to the upper part of ring and locates near to $\text{C}_2\text{--H}$ group of imidazolium cation. However, the anion does not move and only localizes near the $\text{C}_5\text{--H}$ group due to the steric exclusion from alkyl chains in the alkyl-back initial configurations (ethyl-back in Figure 1 and butyl-back in Figure 2). In these optimized conformers of ion pairs, there are more than one $\text{F}\cdots\text{H}$ H-bond between cation and anion. The H-bonds exhibit the major intermolecular structural feature in these ion pairs. The

charges distribution of cation is changed along with the position of anions, while the anion approaches the cation and the small charges transfer from anion to cation.

The DFT-based method underestimates the interaction energies generally at different theoretical levels, and DFT+D method can provide more accurate estimation which is even better than the MP2 method. The energy decomposition by SAPT found that the H-bonds and van der Waals forces are not negligible though the electrostatic attraction is still dominant. In the total energy, the contribution from the electrostatic attraction is 71%, the exchange energy is 14.4%, the induction term is 10%, and the dispersion term is 4.7%, respectively. The NBO delocalization energies of the $n_F \rightarrow \sigma_{C-H}^*$ H-bonds are smaller than those of the protic ionic liquids but larger than the molecular solvents. It indicates a cooperative interaction between H-bonds and electrostatic forces. However, the H-bonded capacities do not show the consistent changes with the interaction energies and the number of H-bonds.

The canonical orbital analysis found that H-bonded interaction is an σ -type orbital overlap. The σ -orbital overlap and the partial charge transfer result in significant energy reduction, and rationalize the preferable location of the anion, which is an essential understanding for the structures of ILs.

The strong agreement between the calculated and experimental IR spectra, even in the far-IR region, indicates that these structures of the ion clusters of $([Emim][BF_4])_n$ exhibit the microscopic structural models for the bulk phase IL, in which cations and anions connect with each other by H-bonds to form a local quasi-3D dimensional network structure in which the cations arrange at the different alternative layers, while the anions are sandwiched between two cations.

Intuitively, the properties of ionic liquids should be determined by the strong Coulomb interactions, and the difference to the high-temperature molten salts (such as NaCl) seems to be melting point. However, the calculation and experimental data have indicated that the H-bonds play more important roles than the pure electrostatic force in locating the positions of ions and determining the properties of ILs.

■ ASSOCIATED CONTENT

S Supporting Information. Figure S1 shows the positions of H-bonded interactions in $EmimBF_4(I)$ and $EmimBF_4(III)$ ion pairs by RDG function. Figure S2 shows the ions clusters of $(EmimBF_4)_n$ with $n = 2, 3, 4, 5$ in tube fashion. The complete text of ref 40 is also given. This material is available free of charge via the Internet at <http://pubs.acs.org>.

■ AUTHOR INFORMATION

Corresponding Author

*E-mail: sjzhang@home.ipe.ac.cn.

■ ACKNOWLEDGMENT

This work was supported by the National Basic Research Program of China (2009CB219900), and the National Natural Scientific Fund of China (20936005, 21073194, and 20903098).

■ REFERENCES

- (1) Rogers, R. D.; Seddon, K. R. *Science* **2003**, *302*, 792–793.
- (2) Zhang, S.; Lu, X.; Zhou, Q.; Li, X.; Zhang, X.; Li, S. *Ionic Liquids: Physicochemical Properties*; Elsevier: New York, 2009.

- (3) Welton, T. *Chem. Rev.* **1999**, *99*, 2071–2083.
- (4) Rogers, R. D. *Nature* **2007**, *447*, 917–918.
- (5) Dymek, C. J.; Grossie, D. A.; Fratini, A. V.; Adams, W. W. *J. Mol. Struct.* **1989**, *213*, 25–34.
- (6) Hitchcock, P. B.; Seddon, K. R.; Welton, T. *J. Chem. Soc., Dalton Trans.* **1993**, 2639–2643.
- (7) Hanke, C. G.; Lynden-Bell, R. M. *J. Phys. Chem. B* **2003**, *107*, 10873–10878.
- (8) Holbrey, J. D.; Reichert, W. M.; Nieuwenhuyzen, M.; Johnston, S.; Seddon, K. R.; Rogers, R. D. *Chem. Commun.* **2003**, 1636–1637.
- (9) Holbrey, J. D.; Reichert, W. M.; Nieuwenhuyzen, M.; Sheppard, O.; Hardacre, C.; Rogers, R. D. *Chem. Commun.* **2003**, 476–477.
- (10) Berg, R. W.; Deetlefs, M.; Seddon, K. R.; Shim, I.; Thompson, J. M. *J. Phys. Chem. B* **2005**, *109*, 19018–19025.
- (11) Yokozeke, A.; Kasprzak, D. J.; Shiflett, M. B. *Phys. Chem. Chem. Phys.* **2007**, *9*, 5018–5026.
- (12) Abdul-Sada, A. K.; Greenway, A. M.; Hitchcock, P. B.; Mohammed, T. J.; Seddon, K. R.; Zora, J. A. *J. Chem. Soc., Chem. Commun.* **1986**, 1753–1754.
- (13) Talaty, E. R.; Raja, S.; Storhaug, V. J.; Dolle, A.; Carper, W. R. *J. Phys. Chem. B* **2004**, *108*, 13177–13184.
- (14) Remsing, R. C.; Wildin, J. L.; Rapp, A. L.; Moyna, G. *J. Phys. Chem. B* **2007**, *111*, 11619–11621.
- (15) Matsumoto, K.; Hagiwara, R. *J. Fluorine Chem.* **2007**, *128*, 317–331.
- (16) Abdul-Sada, A. K.; Greenway, A. M.; Hitchcock, P. B.; Mohammed, T. J.; Seddon, K. R.; Zora, J. A. *J. Chem. Soc., Chem. Commun.* **1986**, 1753–1754.
- (17) Choudhury, A. R.; Winterton, N.; Steiner, A.; Cooper, A. I.; Johnson, K. A. *J. Am. Chem. Soc.* **2005**, *127*, 16792–16793.
- (18) Holbrey, J. D.; Reichert, W. M.; Rogers, R. D. *Dalton Trans.* **2004**, 2267–2271.
- (19) Fumino, K.; Wulf, A.; Ludwig, R. *Angew. Chem., Int. Ed.* **2008**, *47*, 8731–8734.
- (20) Fumino, K.; Wulf, A.; Ludwig, R. *Angew. Chem., Int. Ed.* **2009**, *48*, 3184–3186.
- (21) Wulf, A.; Fumino, K.; Ludwig, R. *Angew. Chem., Int. Ed.* **2010**, *49*, 449–453.
- (22) Weingartner, H. *Angew. Chem., Int. Ed.* **2008**, *47*, 654–670.
- (23) Dong, K.; Zhou, G.; Liu, X.; Yao, X.; Zhang, S. *J. Phys. Chem. C* **2009**, *113*, 10013–10020.
- (24) Zhao, W.; Leroy, F. d.; Heggen, B.; Zahn, S.; Kirchner, B.; Balasubramanian, S.; Müller-Plathe, F. *J. Am. Chem. Soc.* **2009**, *131*, 15825–15833.
- (25) Shah, J. K.; Brennecke, J. F.; Maginn, E. J. *Green Chem.* **2002**, *4*, 112.
- (26) Hanke, C. G.; Price, S. L.; Lynden-Bell, R. M. *Mol. Phys.* **2001**, *99*, 801.
- (27) Morrow, T. I.; Maginn, E. J. *J. Phys. Chem. B* **2002**, *106*, 12807–12813.
- (28) Gutowski, K. E.; Maginn, E. J. *J. Am. Chem. Soc.* **2008**, *130*, 14690–14704.
- (29) Liu, Z. P.; Huang, S. P.; Wang, W. C. *J. Phys. Chem. B* **2004**, *108*, 12978–12989.
- (30) Kowsari, M. H.; Alavi, S.; Ashrafzaadeh, M.; Najafi, B. *J. Chem. Phys.* **2008**, *129*, 224508–224521.
- (31) Lopes, J. N. A. C.; Padua, A. A. H. *J. Phys. Chem. B* **2006**, *110*, 7485–7489.
- (32) Lopes, J. N. C.; Deschamps, J.; Padua, A. A. H. *J. Phys. Chem. B* **2004**, *108*, 2038–2047.
- (33) Vatamanu, J.; Borodin, O.; Smith, G. D. *J. Am. Chem. Soc.* **2010**, *132*, 14825–14833.
- (34) Smith, G. D.; Borodin, O.; Bedrov, D. *J. Phys. Chem. A* **1998**, *102*, 10318–10323.
- (35) Dong, K.; Zhang, S.; Wang, D.; Yao, X. *J. Phys. Chem. A* **2006**, *110*, 9775–9782.
- (36) Hunt, P. A.; Kirchner, B.; Welton, T. *Chem.—Eur. J.* **2006**, *12*, 6762–6775.

- (37) Hunt, P. A.; Gould, I. R. *J. Phys. Chem. A* **2006**, *110*, 2269–2282.
- (38) Buhl, M.; Chaumont, A.; Schurhammer, R.; Wipff, G. *J. Phys. Chem. B* **2005**, *109*, 18591–18599.
- (39) Turner, E. A.; Pye, C. C.; Singer, R. D. *J. Phys. Chem. A* **2003**, *107*, 2277–2288.
- (40) Frisch, M. J.; Trucks, G. W.; Schlegel, H. B.; Scuseria, G. E.; Robb, M. A.; Cheeseman, J. R.; Scalmani, G.; Barone, V.; Mennucci, B.; Petersson, G. A. et al. *Gaussian09 B.01*; Gaussian, Inc.: Wallingford, CT, 2009.
- (41) Schwabe, T.; Grimme, S. *Phys. Chem. Chem. Phys.* **2007**, *9*, 3397–3406.
- (42) Foster, J. P.; Weinhold, F. *J. Am. Chem. Soc.* **1980**, *102*, 7211–7218.
- (43) Reed, A. E.; Weinstock, R. B.; Weinhold, F. *J. Chem. Phys.* **1985**, *83*, 735–746.
- (44) Jezioriski, B.; Moszynski, R.; Szalewicz, K. *Chem. Rev.* **1994**, *94*, 1887–1930.
- (45) Zahn, S.; Bruns, G.; Thar, J.; Kirchner, B. *Phys. Chem. Chem. Phys.* **2008**, *10*, 6921–6924.
- (46) Maddox, J. *Nature* **1989**, *339*, 173–173.
- (47) Kolano, C.; Helbing, J.; Kozinski, M.; Sander, W.; Hamm, P. *Nature* **2006**, *444*, 469–472.
- (48) Marx, D. *Science* **2004**, *303*, 634–636.
- (49) Jr., C. J. D.; Grossie, D. A.; Fratini, A. V.; Adams, W. W. *J. Mol. Struct.* **1989**, *213*, 25–34.
- (50) Liu, Z.; Huang, S.; Wang, W. *J. Phys. Chem. B* **2004**, *108*, 12978–12989.
- (51) Fumino, K.; Wulfa, A.; Ludwig, R. *Phys. Chem. Chem. Phys.* **2009**, *11*, 8790–8794.
- (52) Lehmann, S. B. C.; Roatsch, M.; Schöppke, M.; Kirchner, B. *Phys. Chem. Chem. Phys.* **2010**, *12*, 7473–7486.
- (53) Tsuzuki, S.; Tokuda, H.; Hayamizu, K.; Watanabe, M. *J. Phys. Chem. B* **2005**, *109*, 16474–16481.
- (54) Izgorodina, E. I. *Phys. Chem. Chem. Phys.* **2011**, *13*, 4189–4207.
- (55) Grimme, S. *J. Chem. Phys.* **2006**, *124*, 034108.
- (56) Zahn, S.; Uhlig, F.; Thar, J.; Spickermann, C.; Kirchner, B. *Angew. Chem., Int. Ed.* **2008**, *47*, 3639–3641.
- (57) Sosa, G. L.; Peruchena, N. M.; Contreras, R. H.; Castro, E. A. *J. Mol. Struct.* **2002**, *577*, 219–228.
- (58) Wang, Y.; Voth, G. A. *J. Am. Chem. Soc.* **2005**, *127*, 12192–12193.
- (59) Izvekov, S.; Violi, A.; Voth, G. A. *J. Phys. Chem. B* **2005**, *109*, 17019–17024.
- (60) Liu, X.; Zhou, G.; Zhang, S. *Fluid Phase Equilib.* **2008**, *272*, 1–7.
- (61) Mizuse, K.; Mikami, N.; Fujii, A. *Angew. Chem., Int. Ed.* **2010**, *49*, 10119–10122.
- (62) Roth, C.; Poppel, T.; Fumino, K.; Köckerling, M.; Ludwig, R. *Angew. Chem., Int. Ed.* **2010**, *49*, 10221–10224.
- (63) Matsumoto, K.; Hagiwara, R.; Mazej, Z.; Benkič, P.; Žemva, B. *Solid State Sci.* **2006**, *8*, 1250–1257.
- (64) Hasan, M.; Kozhevnikov, I. V.; Siddiqui, M. R. H.; Femoni, C.; Steiner, A.; Winterton, N. *Inorg. Chem.* **2001**, *40*, 795–800.
- (65) Hardacre, C.; McMath, S. E. J.; Nieuwenhuyzen, M.; Bowron, D. T.; Soper, A. K. *J. Phys.: Condens. Matter* **2003**, *15*, S159.
- (66) Hardacre, C.; Holbrey, J. D.; McMath, S. E. J.; Bowron, D. T.; Soper, A. K. *J. Chem. Phys.* **2003**, *118*, 273–279.
- (67) Qiao, B.; Krekeler, C.; Berger, R.; Site, L. D.; Holm, C. *J. Phys. Chem. B* **2008**, *112*, 1743–1751.
- (68) Canongia Lopes, J. N.; Padua, A. A. H. *J. Phys. Chem. B* **2006**, *110*, 3330–3335.